INFLUENCE OF MEASUREMENT GEOMETRY ON THE OPTICAL PROPERTIES OF CELLULOSE NANOCRYSTAL COATINGS CONTAINING EFFECT PIGMENTS

MIRJAM LESKOVŠEK* and MIRICA KARLOVITS**

*University of Ljubljana, Faculty of Natural Sciences and Engineering, Snežniška 5, SI-1000 Ljubljana, Slovenia
**National Institute of Chemistry, Hajdrihova 19, SI-1000 Ljubljana, Slovenia
✉ Corresponding author: M. Karlovits, mirica.karlovits@ki.si

Received August 21, 2026

Cellulose nanocrystals (CNCs) are promising bio-based materials for functional coatings. This study investigated the influence of measurement geometry on the optical properties of CNC coatings containing four effect pigments with different compositions and particle sizes. Spectral reflectance was measured from 400 to 700 nm at a fixed illumination angle of 45° and six aspecular angles (−15°, 15°, 25°, 45°, 75°, and 110°). Flop Index (FI), Pearson correlation analysis, and scanning electron microscopy (SEM) were also used to evaluate the coatings. The results revealed a pronounced influence of measurement geometry on spectral reflectance, with the highest values generally observed at the near-specular geometry (45as−15°) and decreasing towards the far-aspecular angles. The Flop Index ranged from 6.0 to 9.7, with CNC–EP4 coating showing the strongest angular variation. SEM analysis showed that pigment particle size affected coating morphology, with smaller particles producing a more homogeneous surface. Overall, the results demonstrate the importance of multi-angle measurements for reliable characterisation of CNC coatings containing effect pigments.

Keywords: cellulose nanocrystals, effect pigments, spectral reflectance, Flop Index

INTRODUCTION

In recent years, bio-based nanomaterials have attracted considerable attention as sustainable alternatives to petroleum-derived polymers in advanced functional coatings.[1,2] Cellulose nanocrystals (CNCs), also known as cellulose nanowhiskers or nanocrystalline cellulose, are derived from renewable biomass and offer a sustainable alternative in many applications.[3] CNCs derived from cellulose via acid hydrolysis with their rod-like morphology and high crystallinity can serve as highly effective reinforcing agents in polymer matrices and coatings, significantly improving mechanical performance, barrier properties, and durability.[4,5] These rod-like whiskers, typically 50–500 nm in length and 5–30 nm in diameter, exhibit morphology, crystallinity, and surface chemistry that vary according to their cellulosic source and preparation method, influencing their physicochemical properties.[6]

To expand the visual appearance, and applicability of CNC-based coatings, effect pigments, such as mica-based ones, can be incorporated into the CNC formulation. Special effect pigments are almost exclusively inorganic pigments that provide additional color effects, such as angular color dependence (luster, iridescence, color variability) or texture, when incorporated into coatings, inks, paints, plastics and their subsequent application onto a substrate. The visual appearance originates in reflection and deflection of light at thin single and multiple layers.[7-9] Their pronounced reflective properties result from their anisotropic, platelet-like morphology, which is a key difference from conventional pigments that typically have an isotropic, spherical structure. Due to this anisotropic geometry, effect pigments act like microscopic mirrors, reflecting incident light directly back towards its source and thus producing unique visual effects, and are designed to produce visual appearance, such as the metallic or pearlescent appearances, which have long been associated with goniochromatic effects.[8,10]

Different types of pigment create different appearances in a product. Absorption pigments reflect light of a specific wavelength while absorbing other light, creating a matte color effect. Effect pigments, such as pearl lustre pigments, give a shimmering and glittering impression, enhancing color expression in a product. Pearl lustre pigments consist of a substrate such as mica and a coating such as titanium dioxide (TiO_2), with a substrate layer of metal oxides. Furthermore, interference pigments can be created by changing the thickness of the coating. Using the same coating material, such as TiO_2, reflection and interference from different coating thicknesses create various color expressions.[7]

Effect coatings are commonly measured using multi-angle spectrophotometers with a single illumination angle of 45° and multiple detection angles of -15°, 15°, 25°, 45°, 75° and 110° from the specular reflection (Fig. 1).

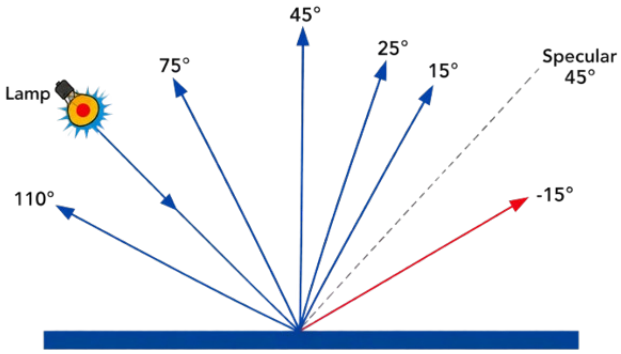


Figure 1: Example of six-angle color measurement

Effect pigments may create very large color shifts as the viewing and illumination angles. Thus, the choice of measurement angles is critical. Colored pigments absorb some of the light that falls on them and reflect the rest of it in a non-directional way. Aluminium pigments reflect the incoming light at a consistent angle and, depending on their type, may create very bright effects.[11]

Recent research has increasingly emphasised the importance of measurement geometry in the characterisation of materials exhibiting angle-dependent optical effects. Goniochromatic materials, including coatings containing interference and multicolor effect pigments, show pronounced variations in spectral reflectance and perceived color as a function of illumination and observation geometry. Recent work by Panahi *et al.*[12] demonstrated that the optical appearance of highly specular goniochromatic materials cannot be adequately described by a single measurement geometry and proposed an improved bidirectional reflectance distribution function (BRDF) model based on separating near-specular and diffuse reflectance components. In parallel, cellulose nanocrystals (CNCs) have attracted considerable attention as sustainable materials with unique optical properties. Their ability to self-assemble into chiral nematic structures can produce structural coloration whose spectral response strongly depends on the orientation of the nanostructure and the observation angle.[3] In addition, recent developments in CNC-based photonic pigments show that cellulose-derived materials can provide pronounced iridescent, angle-dependent optical effects, further enhancing their potential for functional coatings, decorative applications, and anti-counterfeiting technologies.[13]

Despite these advances, only a few studies has been focused on the role of CNCs as a binder matrix for effect pigments and to how measurement geometry influences the resulting optical properties of such coatings. Using multi-angle spectrophotometry, we systematically evaluate the relationships between pigment particle size, surface morphology, and angularly dependent optical response.

EXPERIMENTAL

Materials

For the experimental work, a commercially available aqueous suspension of cellulose nanocrystals (CNCs) was obtained from Nanocrystacell (Slovenia). The suspension had a white-translucent appearance, with a solid content ranging between 2 and 5 wt%. According to the manufacturer's specifications, the CNC particles had an average width of 10–15 nm and a length of 150–300 nm.

To study their optical and aesthetic performance, four different commercial effect pigments (detailed in Table 1) were sourced from Merck and Eckart, both based in Germany. Each pigment was individually incorporated into the CNC suspension at a fixed concentration of 20 wt% relative to the CNC content, followed by thorough homogenisation to ensure uniform dispersion. The formulations were applied onto matte black paper substrates (grammage: 130 g/m²; supplied by Bringmann) to maximise the visual contrast of the effect pigments. Prior to application, the paper sheets were conditioned for 24 hours under controlled standard atmospheric conditions (23 °C and 50% relative humidity, in accordance with ISO 187). Coating was performed using a K Control Coater equipped with a meter bar (wire diameter: 0.05 mm; wet film deposit: 4 μm).

Table 1
Properties of the effect pigments

Label	Form	Color shade	Chemical composition	Particle size
EP1	Powder	Blue	Synthetic calcium aluminum borosilicate (59-77%) coated with titanium dioxide (22-32%), silicone dioxide (1-8%), stannic oxide (≤ 2%)	20–200 μm
EP2	Powder	Blue	Mica (50-70%), titanium dioxide (30-45%), stannic oxide (≤ 1%).	5–35 μm
EP3	Powder	Silver	Titanium dioxide (29-39%), tin oxide (< 1%), synthetic fluorphlogopite (60-71%)	1–15 μm
EP4	Powder	Silver	Titanium dioxide (20-30%), tin oxide (≤ 1%), synthetic fluorphlogopite (69-80%)	10–40 μm

Measurements

Spectral reflectance of the coatings was measured in the spectral region between 400 and 700 nm, using an MA-T12 handheld multi-angle spectrophotometer (manufacturer: X-Rite, Germany) at a fixed illumination angle of 45° and at aspecular angles of -15°, 15°, 25°, 45°, 75°, and 110° under D50 illuminant and 2° standard observer. CIE Lightness (L*) was measured under the same conditions, and on this basis the Flop Index (FI) was calculated.

The surface morphology of the coatings was examined using a Scanning Electron Microscope (JSM-6060 LV, JEOL, Japan), at an accelerating voltage of 10 kV and 200x magnification.

RESULTS AND DISCUSSION

Spectral reflectance of CNC coatings containing effect pigments

Each surface is defined by spectral reflectance, R(λ), a ratio of the reflected light from a sample to that reflected by a pefrect diffuser identically illuminated.[14] When light strikes the surface of a sample, some of it is reflected. At this stage, the reflectance of the sample is defined as the ratio of the luminous flux of light reflected from the sample to the luminous flux of light reflected from a totally diffuse sample (an ideal white sample). As a result, white has the highest reflectance, close to 100%, while black has the lowest. A sample's reflectance is typically independent of the light source and observer, and it can provide a comprehensive description of the sample's color characteristics.[15]

The results of spectral reflectance measurements of CNC coatings containing effect pigments are presented in Figures 2-5.

Figure 2 shows the spectral reflectance of the CNC–EP1 coating measured at a fixed 45° illumination angle across six aspecular angles. Overall, the highest reflectance occurs at the near-specular geometry at 45as-15°, with the highest peak at 410 nm (violet region) reaching R=64.7%. The values then gradually decrease up to 570 nm, after which they rise linearly again, reaching R=53.4% at 700 nm. For the 45as15° measurement geometry, the reflectance spectrum exibits maximum at 430 nm, reaching R=59.9%. Subsequently, the reflectance drops steeply to the value of R=26.7% at 580 nm and than increasing again to R=38.2% at 700 nm. At the medium aspecular angle of 45as25°, there occurrs a sharp drop in reflectance to a maximum of about R≈22%. At the geometries of 45as45°, 45as75°, and 45as110°, the reflectance curves flatten significantly. At the 45as45° mesurement geometry, the reflectance drops to R≈8%, while the 45as75° and 45as110° curves overlap perfectly at a low baseline of R≈4%.

Compared to CNC–EP1, the CNC–EP2 coating (Fig. 3) displays a significantly higher overall spectral reflectance. In the coatings investigated, the coating containing larger effect pigment particles (CNC–EP1) exhibited lower spectral reflectance at the selected measurement geometry. This difference cannot be attributed solely to

particle size, as the measured values are also influenced by platelet orientation, pigment composition, and coating structure. The CNC-EP2 coating exhibits extremely high reflectance intensities near-aspecular angle (45as-15°), with the highest peak at 400 nm (violet region) reaching R=198.8%. A clear dip in reflectance is observed around 580 nm, before it slightly increases towards 700 nm. With increasing aspecular angle (45as45° to 45as110°), reflectance sharply drops below 20%. The higher spectral reflectance observed for CNC–EP2 coatings containing smaller effect pigment particles (5-35 μm), compared with CNC–EP1 coating containing larger particles (20–200 μm), may be attributed to differences in light scattering and to the directional reflection characteristics of the pigment flakes. Smaller particles provide a greater number of pigment–binder interfaces and enable more extensive multiple scattering. In contrast, larger effect pigment platelets tend to produce more directional, specular reflection and pronounced sparkle.[16]

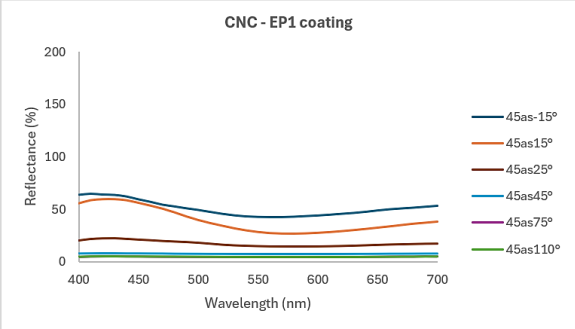


Figure 2: Reflectance spectra of CNC coating containing EP1 pigment, at different measurement geometries

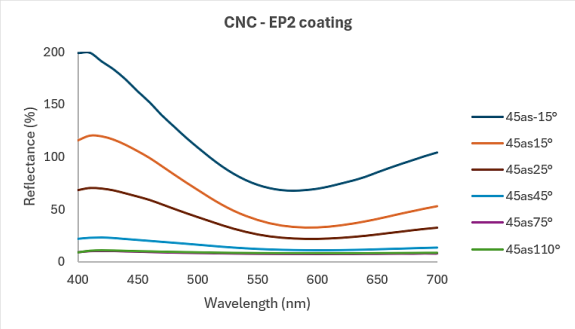


Figure 3: Reflectance spectra of CNC coating containing EP2 pigment, at different measurement geometries

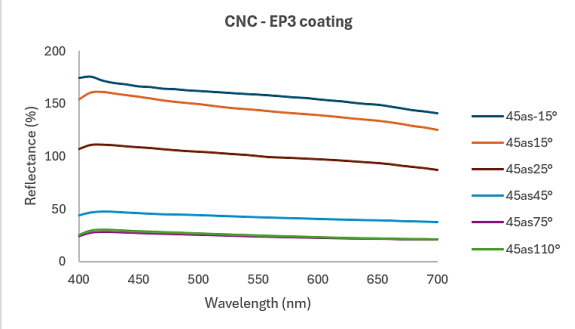


Figure 4: Reflectance spectra of CNC coating containing E3 pigment, at different measurement geometries

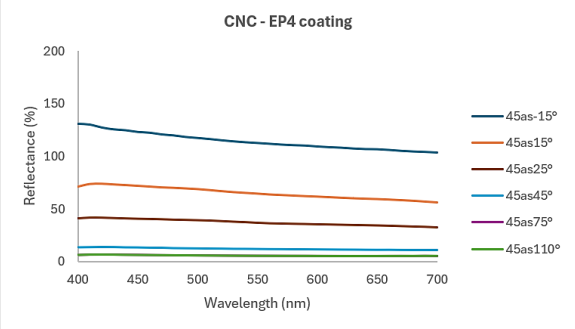


Figure 5: Reflectance spectra of CNC coating containing EP4 pigment, at different measurement geometries

CNC–EP3 coating (Fig. 4) exhibits broad-spectrum high reflectance across the entire visible range (400–700 nm), reaching maximum values of R=175.7% at 410 nm. The spectral profile shows a continuous, gradual decrease from short to long wavelengths, without a characteristic interference minimum. Increasing the aspecular angle results in pronounced lightness flop, with reflectance values decreasing systematically to ~45% at 45as45° and stabilizing near 20%–25% at far-aspecular angles (45as75° and 45as110°).

As shown in Figure 5, similar to the CNC–EP3 coating, the CNC–EP4 coating exhibits a relatively flat, broad-spectrum reflectance profile across the 400–700 nm range, without distinct color interference bands. Maximum reflectance reaches ~130% at 45as-15°. A strong drop is evident as the measured geometry moves to far-aspecular angles, with reflectance rapidly decreasing to below 15% at 45as45° and levelling off around 5% at far-aspecular angles (45as75° and 45as110°).

Table 2 presents Pearson's correlation coefficient, calculated separately for each measurement geometry and each coating, to describe the linear relationship between wavelength and spectral reflectance. The variables were defined as X = wavelength (λ, in nm) and Y = the corresponding spectral reflectance (R(λ), in

%). Each calculation included 31 paired observations within the 400–700 nm range at 10 nm intervals. Thus, the analysis used the complete measured spectrum rather than maximum reflectance values and their corresponding wavelengths. The resulting coefficients are presented in Table 2.

Pearson's correlation coefficient is defined as follows:

$$r = \frac{\sum_{i=1}^{n}((x_i-\bar{x})*(y_i-\bar{y}))}{\sqrt{\sum_{i=1}^{n}(x_i-\bar{x})^2}*\sqrt{\sum_{i=1}^{n}(y_i-\bar{y})^2}} \quad (1)$$

where x_i denotes the wavelength at the i^{th} spectral point, y_i denotes the corresponding reflectance at a fixed measurement geometry, and $\bar{x}$ and $\bar{y}$ are their respective arithmetic means; n = 31. Pearson's correlation coefficient (r) is a statistical measure that quantifies the strength and direction of the linear relationship between two variables. The coefficient ranges from −1 to +1, where +1 indicates a perfect positive linear correlation, −1 indicates a perfect negative linear correlation, and 0 indicates no linear relationship. Generally, absolute values of r greater than 0.7 are considered strong correlations, values between 0.4 and 0.7 indicate moderate correlations, and values below 0.4 represent weak correlations. The variables x_i and y_i relate to individual data points for variables X and Y; $\bar{x}$ and $\bar{y}$ are the means (average) of variable X and variable Y; and the Σ is the "sum of" all corresponding values.[17]

Pearson's correlation analysis showed negative linear associations between wavelength and spectral reflectance for all investigated coatings and measurement geometries (Table 2). CNC–EP3 and CNC–EP4 exhibited strongly negative coefficients, ranging from −0.940 to −0.991 and from −0.906 to −0.993, respectively, consistent with their predominantly decreasing reflectance profiles across the visible range. CNC–EP2 showed coefficients between −0.768 and −0.853, whereas CNC–EP1 exhibited greater variation, from −0.113 to −0.753. The lower absolute coefficients for CNC–EP1 indicate that a linear relationship provides a less complete description of its spectral profiles. In particular, several spectra decrease towards a minimum and subsequently increase at longer wavelengths. At 45as75°, reflectance varies only between 4.48% and 4.85%, despite the low coefficient of r = −0.113. These coefficients describe the wavelength dependence of reflectance within individual spectra and do not directly quantify the magnitude of the response to changes in measurement geometry.

Comparison of the two blue coatings shows that CNC–EP2, containing smaller pigment particles (5–35 μm), exhibits higher absolute Pearson coefficients than CNC–EP1 (20–200 μm) at all measurement geometries. This indicates a stronger linear relationship between wavelength and reflectance, rather than higher reflectance or stronger angular dependence. These differences cannot be attributed solely to particle size, because EP1 and EP2 also differ in substrate composition: EP1 is based on calcium aluminium borosilicate, whereas EP2 is mica-based. Both contain titanium dioxide, but the available compositional information does not establish their optical layer thicknesses or platelet orientation within the coatings. In contrast, the two silver pigments, EP3 and EP4, share a synthetic fluorphlogopite substrate and exhibit similarly strong negative coefficients despite their different particle size ranges. Their predominantly decreasing spectral profiles therefore produce comparable Pearson coefficients.

To assess the non-linearity of the CNC–EP1 and CNC–EP2 spectra, linear, second-order polynomial, and logarithmic models were fitted separately at each measurement geometry using the same 31 wavelength–reflectance pairs. The models were $R(\lambda) = a + b\lambda$, $R(\lambda) = a + b\lambda + c\lambda^2$, and $R(\lambda) = a + b\ \ln(\lambda)$, respectively, with λ expressed in nm. Model performance was evaluated using R^2, adjusted R^2, and RMSE, calculated as the square root of the mean squared residual. The quadratic model yielded higher R^2 and adjusted R^2 and lower RMSE than the linear and logarithmic models for all CNC–EP1 and CNC–EP2 spectra. The comparison of linear and quadratic R^2 values is presented in Table 3.

For CNC–EP1, quadratic R^2 values ranged from 0.631 to 0.947, compared with 0.013–0.567 for the linear model. For CNC–EP2, the corresponding ranges were 0.787–0.980 and 0.589–0.728. For example, for CNC–EP1 at 45as−15°, RMSE decreased from 5.639 to 1.617 reflectance percentage points. These results support the use of a quadratic function as a descriptive approximation of the curved spectral profiles within the measured range. However, improved fitting alone does not establish the physical mechanism responsible for these profiles.

Table 2
Pearson's correlation coefficients (r) between wavelength and spectral reflectance for each CNC coating at each measurement geometry

Measurement geometry	Pearson's correlation coefficient (r)			
	CNC–EP1	CNC–EP2	CNC–EP3	CNC–EP4
45as-15°	-0.597	-0.768	-0.991	-0.982
45as15°	-0.753	-0.832	-0.988	-0.990
45as25°	-0.731	-0.843	-0.987	-0.993
45as45°	-0.509	-0.853	-0.973	-0.979
45as75°	-0.113	-0.827	-0.940	-0.925
45as110°	-0.412	-0.788	-0.947	-0.906

Table 3
Comparison of linear and second-order polynomial fits to the spectral reflectance of CNC–EP1 and CNC–EP2

Measurement geometry	CNC–EP1:	CNC–EP1	CNC–EP2	CNC–EP2
	linear R^2	quadratic R^2	linear R^2	quadratic R^2
45as-15°	0.356	0.947	0.589	0.980
45as15°	0.567	0.908	0.692	0.957
45as25°	0.535	0.868	0.711	0.957
45as45°	0.259	0.868	0.728	0.954
45as75°	0.013	0.631	0.684	0.895
45as110°	0.170	0.685	0.620	0.787

Flop Index of CNC coatings containing effect pigments

The flop effect describes the phenomenon where the physically experienced brightness of metallic effect prints depends on the viewing angle. It varies from extremely bright at or close to the gloss angle to rather dark at inclined angles. The flop behavior of metallic prints is determined in practice by using the brightness contrast of printed surfaces during observation under different viewing angles. The Flop Index (FI) indicates the lightness change at different scattering angles.[9,13,18] Factors affecting flop index are the shape and the size of pigment particles and the way they are laid down. The observational angles are grouped into three categories: "Near Specular": 15° or 25°, "Mid Specular" (or diffuse: 45°), and "Far Specular": 75° or 110° and correlate to the instrumental viewing angles.[19]

Flop Index (FI) as a macro-appearance attribute was calculated through the following formula, in which L* is the lightness at 15°, 45°, and 110° near, mid, and far-aspecular angles, respectively:

$$Flop\ Index\ (FI) = \frac{(L15° - L110°)^{1.11}}{(L45°)^{0.86}} \quad (2)$$

where FI = 0 describes a solid color, while FI = 15–17 indicates a high metallic effect. A higher Flop Index (FI) indicates a more glittering, shinier metallic paint, which provides a better visual impression for the consumer.[18,20] Table 4 shows calculated Flop Index of CNC coatings containing effect pigments.

Table 4
Flop Index of coatings

Color shade	Smaller particles	Larger particles
Blue	EP2: 5-35 μm; FI = 6.0	EP1: 20-200 μm; FI = 7.5
Silver	EP3: 1-15 μm; FI = 6.3	EP4: 10-40 μm; FI = 9.7

The Flop Index values ranged from 6.0 to 9.7 (Table 4). To facilitate interpretation, the coatings were compared in two groups according to pigment color shade: the blue coatings CNC–EP1 and CNC–EP2, and the silver coatings CNC–EP3 and CNC–EP4. Within the blue group, CNC–EP1, containing larger pigment particles (20–200 μm), exhibited a higher FI (7.5) than CNC–EP2 (5–35 μm; FI = 6.0). A similar pattern was observed within the silver group: CNC–EP4 (10–40 μm) exhibited a higher FI (9.7) than CNC–EP3 (1–15 μm; FI = 6.3).

Thus, within both pairs, the coating containing the pigment with the larger particle size range showed a greater angular change in lightness. However, this observation cannot be attributed exclusively to particle size. EP1 and EP2 also differ in chemical composition, while EP3 and EP4 share a synthetic fluorphlogopite substrate, but differ in their composition ranges. Platelet orientation and coating morphology may also contribute to the observed FI differences, although their individual contributions were not quantified in this study.

Surface morphology of CNC coatings containing effect pigments

Figures 6-7 show scanning electron micrographs of coatings. As presented in Table 1, pigment EP1 has the largest particles, with sizes ranging from 20 to 200 μm, whereas pigment EP3 consists of the smallest particles, with the sizes between 1 and 15 μm.

The SEM micrographs (Figs. 6-7) provide a qualitative comparison of pigment distribution and surface morphology within the CNC coatings. CNC–EP1 exhibits prominent overlapping platelet-like structures and a more heterogeneous surface appearance than CNC–EP2. CNC–EP3 shows a comparatively uniform surface morphology. These observations are consistent with the manufacturer-reported particle size ranges in Table 1, although the micrographs were not used to determine quantitative particle size distributions or platelet orientation.

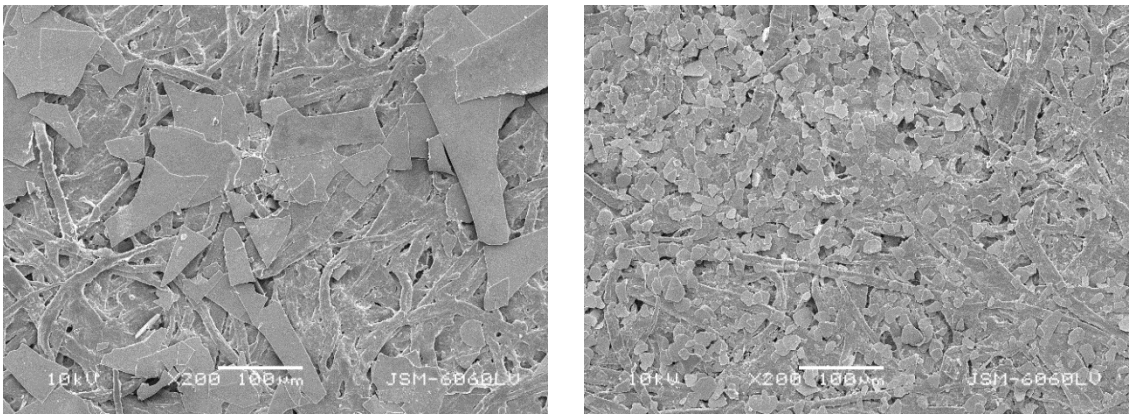


Figure 6: Scanning electron micrographs of coatings: CNC-EP1 (left) and CNC-EP2 (right)

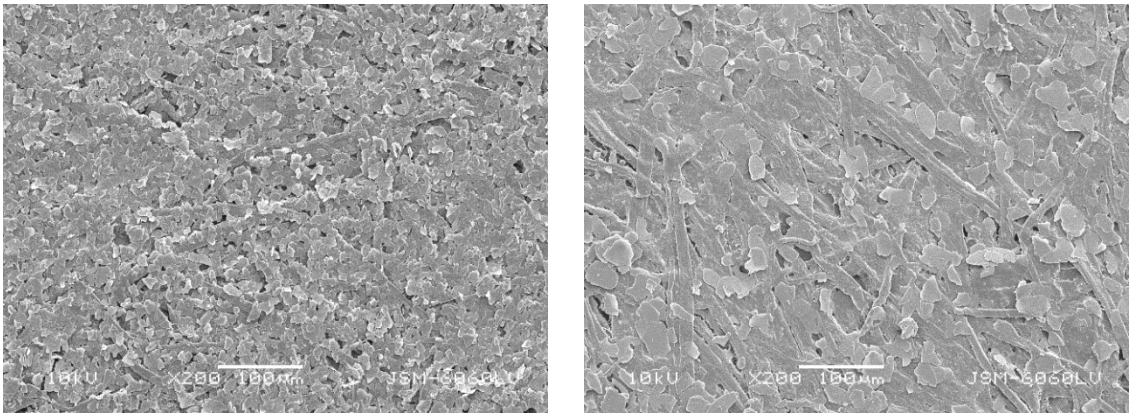


Figure 7: Scanning electron micrographs of coatings: CNC-EP3 (left) and CNC-EP4 (right)

The observed morphology may contribute to these differences because the spatial arrangement and ori entation of reflective platelets affect the distribution of reflected light. However, the present SEM images do not quantify these factors, and their individual effects cannot be established. Pigment composition must also be considered: EP1 and EP2 have different substrates, whereas EP3 and EP4 share a synthetic fluorphlogopite substrate, but differ in their reported composition ranges. The blue and silver spectral profiles are therefore interpreted as the combined response of pigment optical characteristics and coating structure. The SEM observations support a

qualitative association between morphology and optical behaviour, rather than demonstrating that particle size or surface homogeneity alone controls reflectance and FI.

CONCLUSION

Measurement geometry substantially affected the measured spectral reflectance of CNC coatings containing effect pigments. All four coatings exhibited their highest measured reflectance at the near-specular geometry of 45as−15°, with lower values at larger aspecular angles. These results demonstrate the importance of multi-angle measurements for characterising both spectral appearance and angular lightness variation.

The blue coatings, CNC–EP1 and CNC–EP2, exhibited pronounced wavelength-dependent reflectance profiles, whereas the silver coatings, CNC–EP3 and CNC–EP4, showed broader, predominantly decreasing spectra. Quadratic fitting described the CNC–EP1 and CNC–EP2 spectra more accurately than linear fitting, demonstrating that Pearson's coefficient alone provides an incomplete description of their non-linear spectral profiles.

Within both color groups, the coating containing the pigment with the larger particle size range exhibited a higher Flop Index: 7.5 for CNC–EP1 compared with 6.0 for CNC–EP2, and 9.7 for CNC–EP4 compared with 6.3 for CNC–EP3. Conversely, CNC–EP2 and CNC–EP3 exhibited higher near-specular reflectance than their respective counterparts. Thus, higher reflectance at an individual geometry did not necessarily correspond to greater angular lightness variation.

SEM observations revealed differences in surface morphology, including prominent overlapping platelets in CNC–EP1 and a comparatively uniform surface in CNC–EP3. However, these observations were qualitative, and particle shape, size distributions, and platelet orientation were not quantified. Differences in pigment composition must also be considered, particularly between EP1 and EP2, which have different substrate materials. Although EP3 and EP4 share a synthetic fluorphlogopite substrate, their reported composition and particle size ranges differ. The observed optical behaviour therefore reflects the combined characteristics of the pigment–coating systems; the individual contribution of particle size cannot be isolated from the present results.

Overall, CNCs served as a bio-based matrix for coatings retaining the angle-dependent optical response of the incorporated effect pigments. The findings support evaluating spectral reflectance, angular lightness variation, and coating morphology together when comparing these systems.

REFERENCES

[1] T. Bejoy, C. Raj Midhun, K. B. Athira, M. H. Rubiyah, J. Jithin *et al*., *Chem. Rev*., **118**, 11575 (2018), https://doi.org/10.1021/acs.chemrev.7b00627

[2] D. Trache, A. F. Tarchoun, M. Derradji, T. S. Hamidon, N. Masruchin *et al*., *Frontiers Chem*., **8**, 392 (2020), https://doi.org/10.3389/fchem.2020.00392

[3] B. Frka-Petesic, T. G. Parton, C. Honorato-Rios, A. Narkevicius, K. Ballu *et al*., *Chem. Rev*., **123**, 12595 (2023), https://doi.org/10.1021/acs.chemrev.2c00836

[4] N. Straub, S. Veigel, J. Janesch, C. Lointier, C. Gusenbauer *et al*., *Progress Org. Coat*., **213**, 109919 (2026), https://doi.org/10.1016/j.porgcoat.2025.109919

[5] Y. Xu, Z. Wu, A. Li, N. Chen, J. Rao *et al*., *Polymers*, **16**, 423 (2024), https://doi.org/10.3390/polym16030423

[6] L. Zhang, N. Ren, J. Zhang, X. Gao, M. Cui *et al*., *Chem. Eng. J.*, **509**, 161190 (2025), https://doi.org/10.1016/j.cej.2025.161190

[7] G. Pfaff, *ChemTexts*, **8**, 15 (2022), https://doi.org/10.1007/s40828-022-00166-1

[8] B. Mahltig, J. Zhang, L. Wu, D. Darko, M. Wendt *et al*., *J. Coat. Technol. Res*., **14**, 35 (2017), https://doi.org/10.1007/s11998-016-9854-9

[9] G. Pfaff, "Inorganic Pigments", Walter de Gruyter GmbH, Berlin, 2nd ed., 2023, pp. 242–280

[10] F. Ameri and M. Safi, *J. Coat. Technol. Res*., **23**, 1553 (2026), https://doi.org/10.1007/s11998-025-01199-0

[11] W. R. Cramer and W. M. Cramer, *PCI Paint&Coatings Industry*, accessed August 17, 2026, https://www.pcimag.com/articles/113954-a-new-way-to-visually-evaluate-color

[12] B. Panahi, I. Farup and A. Sole, *Optics Express*, **33**, 38268 (2025), https://doi.org/10.1364/OE.568761

[13] M. S. Vlad-Cristea, V. Landry, P. Blanchet and C. Ouellet-Plamondon, *Int. Scholar. Res. Notices*, **2013**, 930236 (2013), https://doi.org/10.1155/2013/930236

[14] R. Shamey (Ed.), "Encyclopedia of Color Science and Technology", Springer, Cham, 2023, pp. 246–247, https://doi.org/doi.org/10.1007/978-3-030-89862-5

[15] Linshang Technology, *Spectral Reflectance, Metamerism and Whiteness*, accessed August 17, 2026, https://www.linshangtech.com/tech/spectral-reflectance-metamerism-and-whitenes-introduction-tech1479.html

[16] F. J. Maile, G. Pfaff and P. Reynders, *Progress Org. Coat*., **54**, 150 (2005), https://doi.org/10.1016/j.porgcoat.2005.07.003

[17] T. Fu, X. Tang, Z. Cai, Y. Zuo, Y. Tang *et al*., *Progress Org. Coat*., **139**, 105459 (2020), https://doi.org/10.1016/j.porgcoat.2019.105459

[18] S. Fashandi, K. Ansari, M. Mohseni, H. Yahyaei and A. Mansouri, *Optics Express*, **33**, 12673 (2025), https://doi.org/10.1364/oe.553948
[19] M. Karlovits, B. Likozar and U. Novak, *Procs*. *7th International Conference on Technologies & Business Models for Circular Economy Conference*, University of Maribor, Maribor, Slovenia, 2025, pp. 41-49, https://press.um.si/index.php/ump/en/catalog/book/949
[20] L. Shu-Ting, W. Hong-Zhang and L. Jing, *Science China Technological Sciences*, **62**, 1577 (2019), https://doi.org/10.1007/s11431-019-9513-5